

Directional transport of active particles confined in 3D smooth corrugated channel

Bing Wang

School of Mechanics and Optoelectronics Physics, Anhui University of Science and Technology, Huainan, 232001, P.R.China

Abstract

The transport phenomenon of active particles confined in three dimensional corrugated confined channel with Gaussian noises is investigated. Proper noise intensity perpendicular to the symmetry axis is good at the directional transport along the symmetry axis. The generalized resonance transport phenomenon appears with increasing noise intensity parallel to symmetry axis. Transport reverse phenomenon appears with increasing self-propelled speed v_0 .

Keywords: Active Particles, Confined Channel, Directional Transport

1. Introduction

Active particles are able to take up energy from environment and convert the energy to directional motion. Investigation of active particles system has enabled to mimic and dissect mechanisms in biological systems[1]. These investigations have grown substantially both in theory and application[2, 3, 4, 5, 6, 7, 8, 9], especially, particles confined in spatial space. There are numerous realizations of confine active particles in nature ranging from bacteria and spermatozoa to artificial colloidal micro-swimmers, e.g., biological cells[10, 11], ion channels[12], nanoporous materials[13, 14], zeolites[15], microfluidic channels[16], artificial nanopores[17], and ionpumps [18].

Confined active particles shows a series of interesting phenomenons, e.g. current reversal[19, 20, 21], self-organization[22, 23] and so on. Ghosh *et*

Email address: hnitwb@163.com (Bing Wang)

al. investigated active overdamped microswimmers in a two-dimensional periodically compartmentalized channel and proved that ratcheting of Janus particles can be orders of magnitude stronger than for ordinary thermal potential ratchets and thus experimentally accessible[28]. Ao *et al.* investigated the transport diffusivity of Janus particles in the absence of external biases with reflecting walls and found the self-diffusion can be controlled by tailoring the compartment geometry[24]. Bechinger *et al.* given an overview of experimental achievements connected to the realization of artificial microswimmers and nanoswimmers[25]. Murali *et al.* showed that geometric constraints are a route to affect the emergent noise properties of a single active particle[26]. Liu *et al.* investigated the entropic stochastic resonance when a self-propelled Janus particle moves in a double-cavity container[27]. Li *et al.* studied the transport of noninteracting anisotropic particles in a narrow two dimensional left-right and up-down asymmetrical channel[29]. Pototsky *et al.* considered a colony of point like self-propelled surfactant particles without direct interactions that cover a thin liquid layer on a solid support[30].

Previous research considers the particles confined in two dimensions ($2D$) corrugated channel. In this paper, we investigate the directional transport of active particles confined in a three dimensions($3D$) corrugated channel. The paper is structured as follows. Section 2 gives the model considered in this paper. Section 3 analyses the effects of the channel and noise on the system. A concluding discussion is offered in section 4.

2. Basic model and methods

In this work, we consider active particles confined in a $3D$ smooth corrugated channel with Gaussian white noises. The dynamic of the particle is governed by the following dimensionless equations[31, 32, 33]

$$\frac{\partial x}{\partial t} = v_0 \sin \theta(t) \cos \varphi(t) + \xi_x(t), \quad (1)$$

$$\frac{\partial y}{\partial t} = v_0 \sin \theta(t) \sin \varphi(t) + \xi_y(t), \quad (2)$$

$$\frac{\partial z}{\partial t} = v_0 \cos \theta(t) + \xi_z(t), \quad (3)$$

$$\frac{\partial\theta(t)}{\partial t} = \xi_\theta(t), \quad (4)$$

$$\frac{\partial\varphi(t)}{\partial t} = \xi_\varphi(t). \quad (5)$$

Here, v_0 is the self-propelled speed of the particle. The polar angle between v_0 and the z axis is $\theta(t)$. The azimuth angle between projection of v_0 on xoy plane with x axis is $\varphi(t)$. ξ_x , ξ_y and ξ_z are the noises and parallel to x axis, y axis and z axis, respectively. ξ_θ and ξ_φ are the angle noises, respectively. $\xi_i (i = x, y, z, \theta, \varphi)$ satisfies the following relations.

$$\langle \xi_i(t) \rangle = 0, (i = x, y, z, \theta, \varphi), \quad (6)$$

$$\langle \xi_i(t)\xi_j(s) \rangle = \delta_{ij}Q_i\delta(t-t'), (i = x, y, z, \theta, \varphi), \quad (7)$$

$\langle \dots \rangle$ denotes an ensemble average over the distribution of the random forces. $Q_i (i = x, y, z, \theta, \varphi)$ is the noise intensity.

The particles are confined in a 3D smooth corrugated channel. The channel is periodic in space along the z -axis as shown in Fig.1. The wall of the cavity has been modeled by the following sinusoidal function

$$W(z) = \varepsilon[\sin(\frac{2\pi z}{L}) + \frac{\Delta}{4}\sin(\frac{4\pi z}{L})] + f. \quad (8)$$

The shape of the channel are controlled by the parameters ε and f . The adjust parameter of the channel is Δ .

A central practical question in the theory of Brownian motors is the over all long time behavior of the particle, and the key quantities of particle transport is the particle velocity $\langle V \rangle$. Because particles along the x and y directions are confined, we only calculate the z direction average velocity

$$\langle V \rangle = \lim_{t \rightarrow \infty} \frac{\langle z(t) - z(t_0) \rangle}{t - t_0}, \quad (9)$$

$z(t_0)$ is the position of particles at time t_0 .

3. Results and discussion

In this letter, we demonstrate the transport phenomenon of active particles confined in a 3D smooth corrugated channel. In order to give a clear

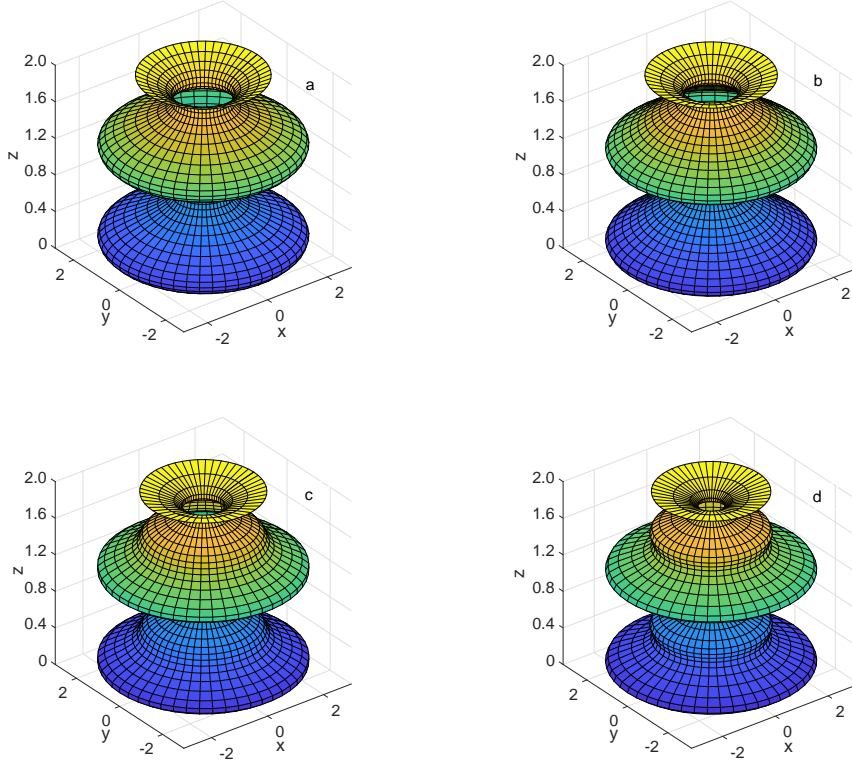


Figure 1: Illustrations of the smooth 3D corrugated channel with $L = 1.0$, $\varepsilon = 1.0$, $f = 1.8$ and (a) $\Delta = 0.0$, (b) $\Delta = 0.8$, (c) $\Delta = 1.6$, (d) $\Delta = 2.4$.

analysis of the system. Eqs.(1, 2, 3, 4, 5) are integrated using the Euler algorithm. The integration step time $\Delta t = 10^{-4}$ and the total integration time is more than 10^5 . The stochastic averages are obtained as ensemble averages over 10^5 trajectories.

The average velocity $\langle V \rangle$ as a function of x axis noise intensity Q_x is reported in Fig.2. In Fig.2(a), we find the particle moves in $-z$ direction($\langle V \rangle < 0$), and $\langle V \rangle$ decreases with increasing Q_x , and the slope of $\langle V \rangle - Q_x$ curve decreases with increasing Q_x and changes to zero when Q_x is large. So small x axis noise intensity will inhibit $-z$ directional transport, proper large x axis noise intensity is good at the $-z$ directional transport, but the effect will become weak when the x axis noise intensity is too large. In Fig.2(b), the average velocity $\langle V \rangle$ ($\langle V \rangle > 0$) increases with increasing Q_x . The slope

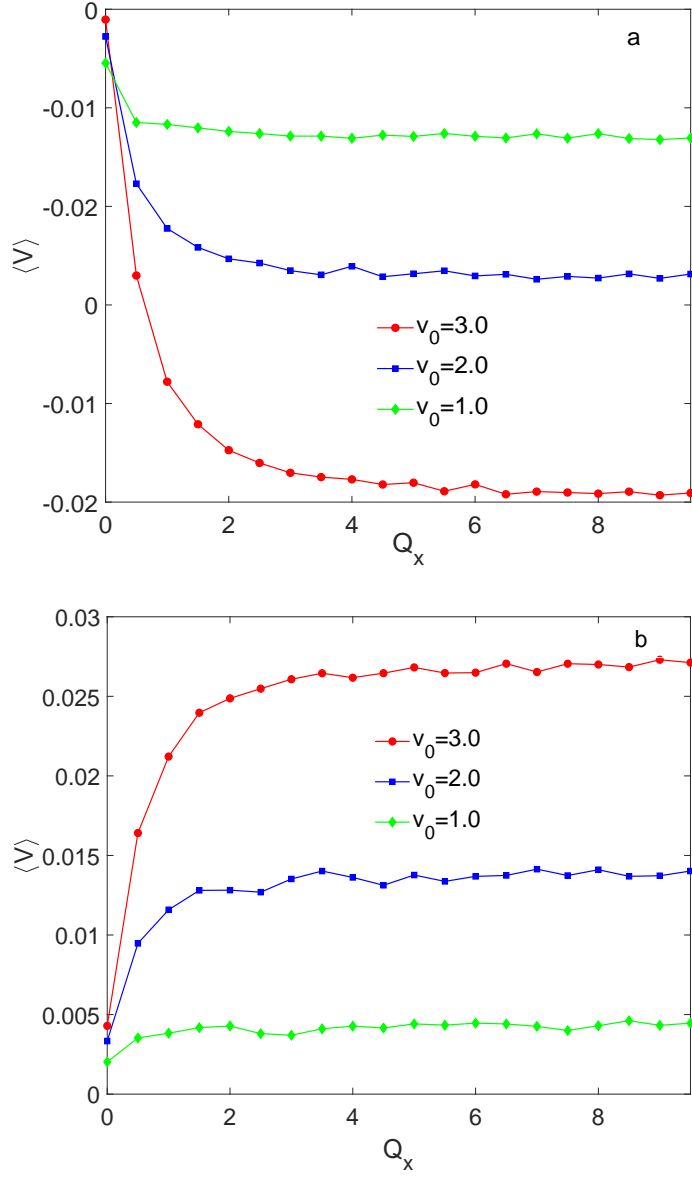


Figure 2: The average velocity $\langle V \rangle$ as a function of Q_x for different self-propelled speed v_0 . The other parameters are $L = 1.0$, $\varepsilon = 1.0$, $f = 1.8$, $Q_y = Q_z = 1.0$, $Q_\theta = Q_\varphi = 0.5$ and (a) $\Delta = -0.8$, (b) $\Delta = 0.8$.

of $\langle V \rangle - Q_x$ curve decreases with increasing Q_x and changes to zero when Q_x is large. So, small x axis noise intensity will inhibit the $+z$ directional transport, and proper large x axis noise intensity is good at the this phenomenon. In Fig.2, we find negative Δ will induce $-z$ directional transport, but positive Δ will induce $+z$ directional transport. Proper large x axis noise intensity is good at the the $-z$ or $+z$ directional transport.

The average velocity $\langle V \rangle$ as a function of y axis noise intensity Q_y is reported in Fig.3. Just like the effect of Q_x (Fig.2), when $\Delta = -0.8$ (Fig.3(a)), the particle moves in the $-z$ direction, and $\langle V \rangle$ monotonic decreases with increasing Q_y , and the $\langle V \rangle - Q_y$ curve changes to horizon when Q_y is large. When $\Delta = 0.8$ (Fig.3(b)), the particle moves in $+z$ direction, and $\langle V \rangle$ monotonic increases with increasing Q_y , and the $\langle V \rangle - Q_y$ curve changes to horizon when Q_y is large. Proper large y axis noise intensity will help to directional transport in $-z$ or z direction, but the effect will become weak when the noise intensity is large. From Figs.2 and 3, we find x axis noise and y axis noise have the same effect on the system. The reason is that the channel is axis-symmetric, and x axis noise and y axis noise are equivalent for the system. From figures 2 and 3, we know that noises perpendicular to the symmetry axis have non-negligible influence on the transport along the symmetry axis.

The average velocity $\langle V \rangle$ as a function of z axis noise intensity Q_z is reported in Fig.4. Unlike the effects of Q_x and Q_y , we find the average speed $|\langle V \rangle|$ has an obvious maximum with increasing Q_z ($\langle V \rangle < 0$ when $\Delta = -0.8$, and $\langle V \rangle > 0$ when $\Delta = 0.8$). So the generalized resonance transport phenomenon appears in the system. There exist an optimum value of noise intensity Q_z , and the directional transport phenomenon is very obvious at this point. Too large or too small Q_z will inhibit the transport in the direction of $-z$ and z .

The average velocity $\langle V \rangle$ as a function of polar angle noise intensity Q_θ is reported in Fig.5. We find whenever $\Delta = -0.8$ or $\Delta = 0.8$, $\langle V \rangle$ monotonic decreases with increasing Q_θ , and $\langle V \rangle > 0$ when Q_θ is small ($Q_\theta < 0.05$). So the particle moves in $+z$ direction when the polar angle noise intensity is small. When $\Delta = -0.8$ (Fig.5(a)), the transport changes from in z direction to in $-z$ direction with increasing Q_θ . So the transport reverse phenomenon appears with increasing Q_θ when $\Delta = -0.8$. But when $\Delta = 0.8$, the particle moves always in $+z$ direction, and the speed becomes smaller and smaller with increasing Q_θ . The transport reverse phenomenon will not appear in this case.

The average velocity $\langle V \rangle$ as a function of the azimuth angle noise inten-

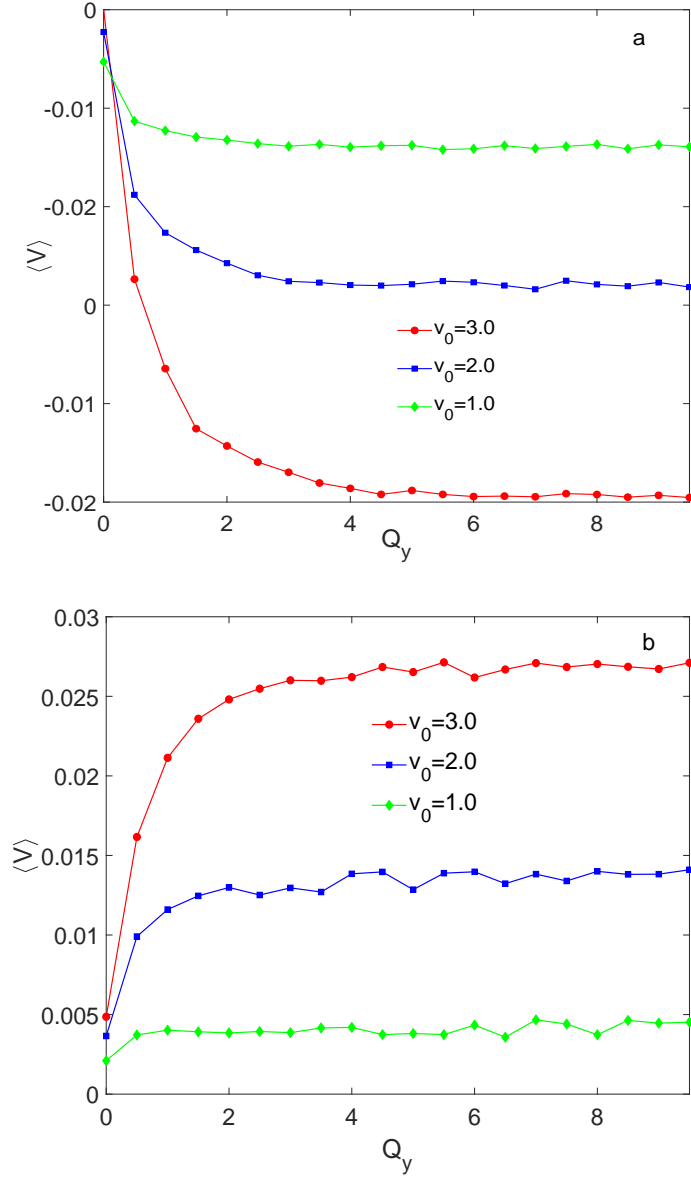


Figure 3: The average velocity $\langle V \rangle$ as a function of Q_y for different self-propelled speed v_0 . The other parameters are $L = 1.0$, $\varepsilon = 1.0$, $f = 1.8$, $Q_x = Q_z = 1.0$, $Q_\theta = Q_\varphi = 0.5$ and (a) $\Delta = -0.8$, (b) $\Delta = 0.8$.

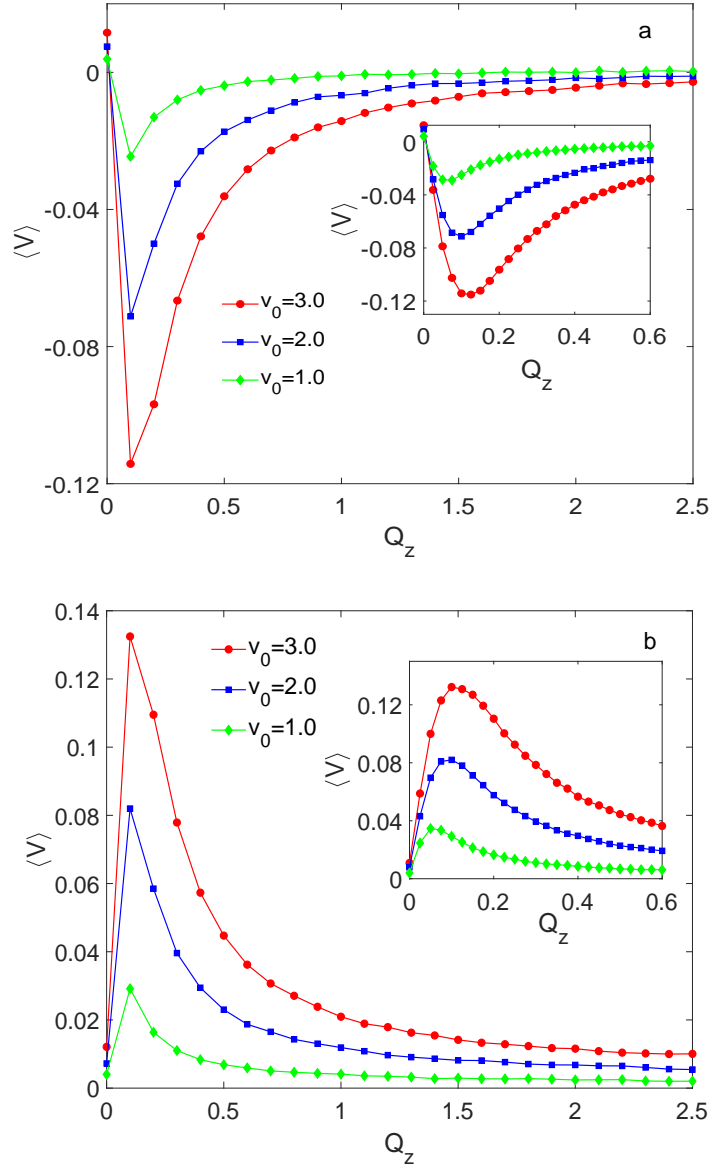


Figure 4: The average velocity $\langle V \rangle$ as a function of Q_z for different self-propelled speed v_0 . The other parameters are $L = 1.0$, $\varepsilon = 1.0$, $f = 1.8$, $Q_x = Q_y = 1.0$, $Q_\theta = Q_\varphi = 0.5$ and (a) $\Delta = -0.8$, (b) $\Delta = 0.8$.

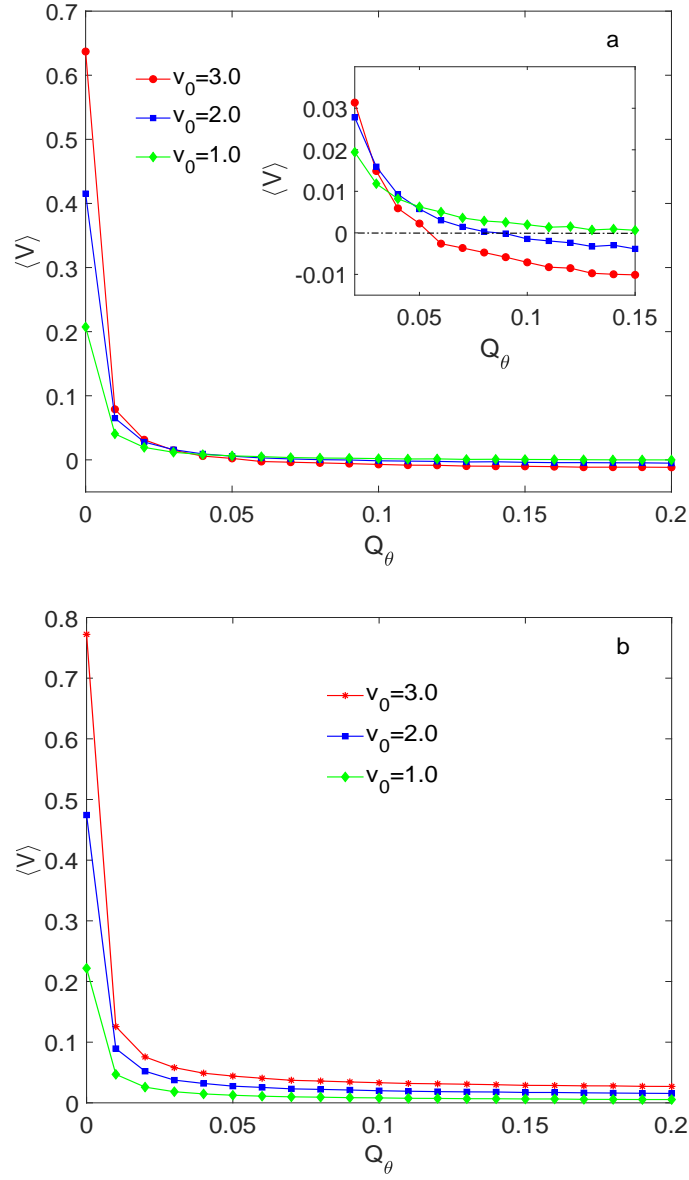


Figure 5: The average velocity $\langle V \rangle$ as a function of polar angle noise intensity Q_θ for different self-propelled speed v_0 . The other parameters are $L = 1.0$, $\varepsilon = 1.0$, $f = 1.8$, $Q_x = Q_y = Q_z = 1.0$, $Q_\varphi = 0.5$ and (a) $\Delta = -0.8$, (b) $\Delta = 0.8$.

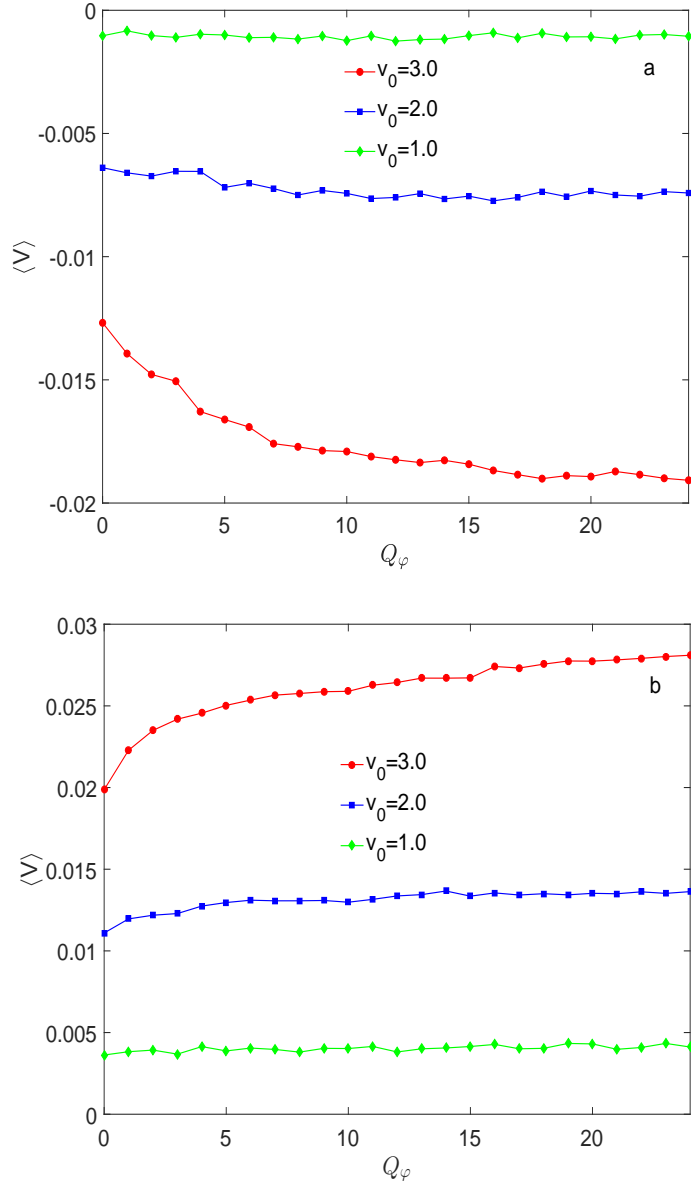


Figure 6: The average velocity $\langle V \rangle$ as a function of azimuth angle noise intensity Q_φ for different self-propelled speed v_0 . The other parameters are $L = 1.0$, $\varepsilon = 1.0$, $f = 1.8$, $Q_x = Q_y = Q_z = 1.0$, $Q_\theta = 0.5$ and (a) $\Delta = -0.8$, (b) $\Delta = 0.8$.

sity Q_φ is reported in Fig.6. We find the average speed $|\langle V \rangle|$ increases with increasing noise intensity Q_φ , so large azimuth angle noise intensity will help to the directional transport in the $-z$ or z direction. We can also find that $\langle V \rangle - Q_\varphi$ curve changes to horizon when Q_φ is large.

The average velocity $\langle V \rangle$ as a function of self-propelled speed v_0 with different the adjust parameter Δ is reported in Fig.7. In Fig.7(a), the average velocity $\langle V \rangle$ exist a minimum and a maximum with increasing self-propelled speed v_0 . The particle moves along $-z$ direction when v_0 is small, and reaches a minimum, then increases with increasing v_0 and reaches a maximum, and decreases with increasing v_0 again. In Fig.7(b), we find $\langle V \rangle > 0$ and $\langle V \rangle$ has a maximum with increasing self-speed v_0 . In this figure, we can also find $\langle V \rangle \rightarrow 0$ when $v_0 = 0$, so the directional transport phenomenon is vary weak for inert particle.

The average velocity $\langle V \rangle$ as a function of the adjust parameter Δ is reported in Fig.8. We find $\langle V \rangle$ first decreases with increasing Δ and reaches a minimum, then increases with increasing Δ and reaches a maximum, then decreases with increasing Δ in the end. There exist a minimum and a maximum in the $\langle V \rangle - \Delta$ curve, so proper value of Δ is good at the z directional transport. Too large or too small Δ will restrain the z directional transport. The transport reverse phenomenon appears with increasing Δ .

4. Conclusions

In this paper, we numerically investigated the transport phenomenon of active particles confined in a $3D$ smooth channel with Gaussian white noises. We find the moving speed along symmetry axis increases with increasing noise intensity perpendicular to the symmetry axis. The average speed has a maximum with increasing noise intensity parallel to the symmetry axis. The adjust parameter has an important influence in the moving direction of the particle. The transport reverse phenomenon will appear with increasing polar angle noise intensity when the adjust parameter is negative.

5. Acknowledgments

Project supported by Natural Science Foundation of Anhui Province(Grant No:1408085QA11) and College Physics Teaching Team of Anhui Province(Grant No:2019jxtd046).

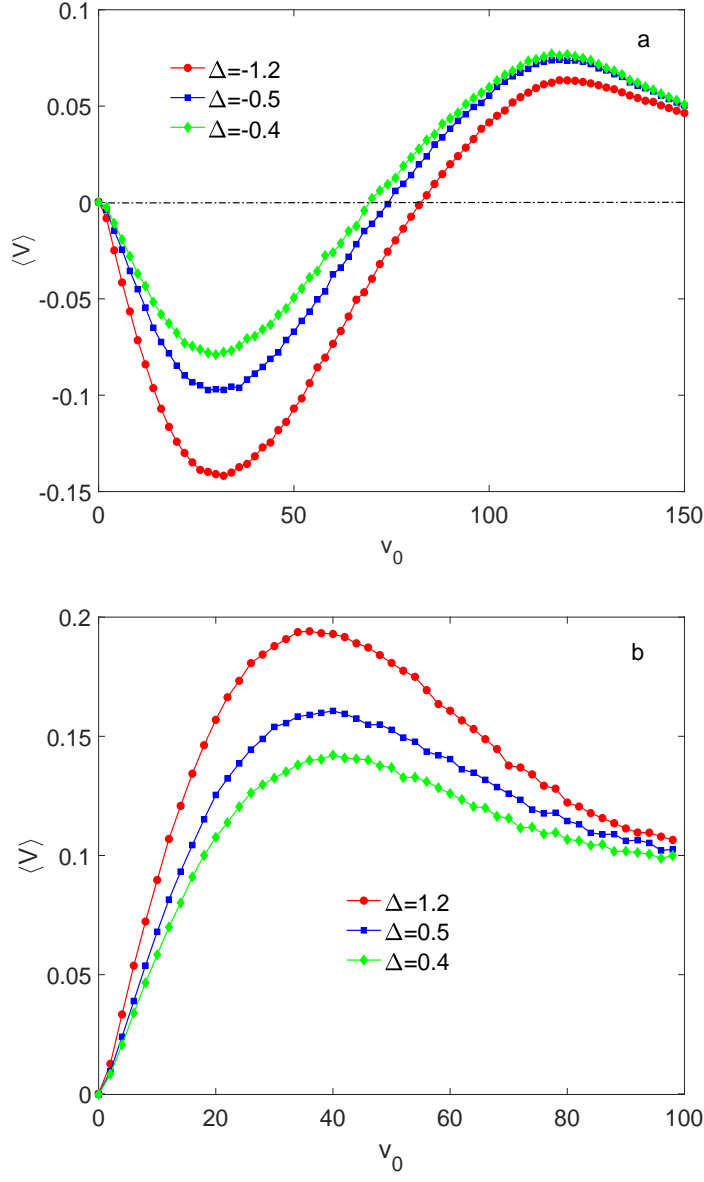


Figure 7: The average velocity $\langle V \rangle$ as a function of v_0 for different Δ . The other parameters are $L = 1.0$, $\varepsilon = 1.0$, $f = 1.8$, $Q_x = Q_y = Q_z = 1.0$, $Q_\theta = Q_\varphi = 0.5$.

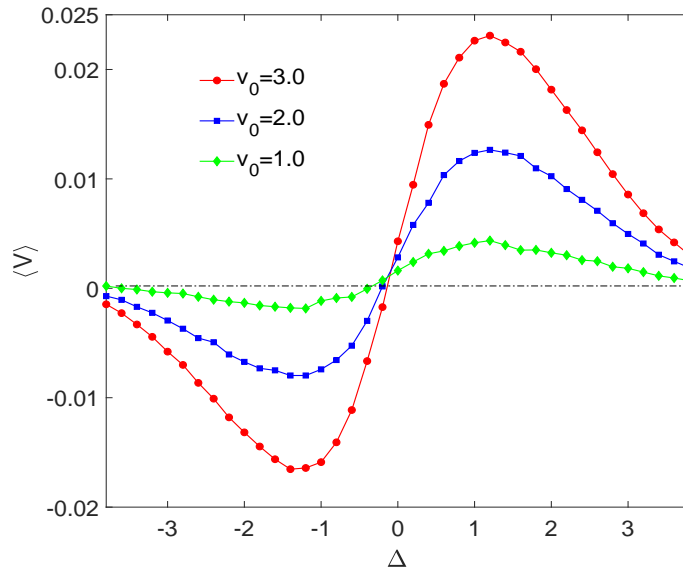


Figure 8: The average velocity $\langle V \rangle$ as a function of adjust parameter Δ for different self-propelled speed v_0 . The other parameters are $L = 1.0$, $\varepsilon = 1.0$, $f = 1.8$, $Q_x = Q_y = Q_z = 1.0$, $Q_\theta = Q_\varphi = 0.5$.

References

- [1] S. Ramaswamy, *Annu. Rev. Condens. Matter Phys.* 1 (2010) 323.
- [2] M. C. Marchetti, J. F. Joanny, S. Ramaswamy, et al., *Rev. Mod. Phys.* 85 (2013) 1143.
- [3] D. Needleman, Z. Dogic, *Nat. Rev. Mater.* 2 (2017) 17048.
- [4] E. Pince, S. K. P. Velu, A. Callegari, et al., *Nat. Commun.* 7 (2016) 10907.
- [5] S. Palagi, P. Fischer, *Nat. Rev. Mater.* 3 (2018) 113.
- [6] P. Pietzonka, E. Fodor, C. Lohrmann, M. E. Cates, U. Seifert, *Phys. Rev. X* 9 (2019) 041032.
- [7] A. Kulkarni, S. P. Thampi, M. V. Panchagnula, *Phys. Rev. Lett.* 122 (2019) 048002.
- [8] J. C. Moreno, M. L. Rubio Puzzo, W. Paul, *Phys. Rev. E* 102 (2020) 022307.
- [9] G. Gompper, R. G. Winkler, T. Speck, A. Solon, C. Nardini, F. Peruani, et al., *J. Phys.: Condens. Matter* 32 (2020) 193001.
- [10] S. Tang, F. Zhang, H. Gong, F. Wei, J. Zhuang, et al., *Sci. Robot.* 5 (2020) eaba6137.
- [11] H. X. Zhou, G. Rivas, A. P. Minton, *Annu. Rev. Biophys.* 37 (2008) 375.
- [12] B. Hille. *Ion Channels of Excitable Membranes*. Sinauer Associates, 3rd edition, 2001. ISBN 0878933212.
- [13] E. Beerdsen, D. Dubbeldam, B. Smit, *Phys. Rev. Lett.* 95 (2005) 164505.
- [14] E. Beerdsen, D. Dubbeldam, B. Smit, *Phys. Rev. Lett.* 96 (2006) 044501.
- [15] F. J. Keil, R. Krishna, M. O. Coppens, *Rev. Chem. Eng.* 16 (2000) 71.
- [16] T. M. Squires, S. R. Quake, *Rev. Mod. Phys.* 77 (2005) 977.
- [17] D. Pedone, M. Langecker, G. Abstreiter, U. Rant. *Nano Lett.* 11(2011) 1561.

- [18] Z. Siwy, I. D. Kosinska, A. Fulinski, C. R. Martin, *Phys. Rev. Lett.* 94 (2005) 048102.
- [19] C. Hu, Y. Ou, J. Wu, Q. Chen, B. Ai, *J. Stat. Mech.* 2015 (2015) 05025.
- [20] H. W. Hu, L. Du, L. H. Qu, Z. L. Cao, Z. C. Deng, Y. C. Lai, *Phys. Rev. Research* 3 (2021) 033162.
- [21] B. Wang, H. Chen, Y. Wu, *Physica A* 537 (2020) 122779.
- [22] J. Richardi, M. P. Pileni, J. J. Weis, *J. Chem. Phys.* 130 (2009) 124515.
- [23] C. Iss, D. Midou, A. Moreau, D. Held, et al., *Soft Matter* 15 (2019) 2971.
- [24] X. Ao, P. K. Ghosh, Y. Li, G. Schmid, P. Hänggi, F. Marchesoni, *EPL* 109 (2015) 10003.
- [25] C. Bechinger, R. Di Leonardo, H. Löwen, C. Reichhardt, G. Volpe, G. Volpe, *Rev. Mod. Phys.* 88 (2016) 045006.
- [26] A. Murali, P. Dolai, A. Krishna, K. Vijay Kumar, S. Thutupalli, *Phys. Rev. Research* 4 (2022) 013136.
- [27] Z. Liu, L. Du, W. Guo, D. Mei, *Eur. Phys. J. B* 89 (2016) 222.
- [28] P. K. Ghosh, V. R. Misko, F. Marchesoni, F. Nori, *Phys. Rev. Lett.* 110 (2013) 268301.
- [29] F. Li, B. Ai, *Physica A* 484 (2017) 27.
- [30] A. Pototsky, U. Thiele, H. Stark, *Eur. Phys. J. E* 39 (2016) 51.
- [31] P. Hänggi, F. Marchesoni, S. Savelev, G. Schmid, *Phys. Rev. E* 82 (2010) 041121.
- [32] Y. Han, A. M. Alsayed, M. Nobili, J. Zhang, T. C. Lubensky, A. G. Yodh, *Science* 314 (2006) 626.
- [33] M. Pu, H. Jiang, Z. Hou, *Soft Matter* 13 (2017) 4112.